Journal of Additive Manufacturing Technologies
DOI: 10.18416/JAMTECH.2111555

Infinite Science | Publishing

Investigating cause of the dissimilar ductility of Inconel 718 fabricated by electron beam melting (EBM)

C. Unver[1,2*], A. Urkmez[2], G.M. Bilgin[2], A. Orhangul[2], D. Turan[1] and S. Turan[1]

[1] Materials Science and Engineering, Eskisehir Technical University, Eskisehir, Turkey
[2] Tusas Engine Industries INC., Eskisehir, Turkey
[*] Corresponding author, email: caglarunver@eskisehir.edu.tr

Abstract

Additive manufacturing has become mainstream many areas. In recent years, aviation has been one of the leading industries using additive manufacturing. While generally metal materials are used in this sector, the production of metal materials with additive manufacturing can be in different ways. Electron beam melting (EBM) method is based on the powder bed fusion (PBF) principle. Using PBF, it is possible to produce parts that are difficult to produce by traditional methods. In this study, it is aimed to explain the different ductility behavior of IN718 produced by EBM method by phase analysis. When all the tensile test results are examined, it is seen that the final tensile strength and yield strength results decreased by about 3%, the area reduction was reduced by about 65%, and the decrease between the elongation results after fracture was 85%. The fracture surfaces were examined different phase images were seen in the samples with value of low ductility. To understand this difference, fracture surfaces and shiny surfaces were examined with electron microscopy and XRD. As a result of the examination, differences were observed in the areas with high Nb content and in the amount of a precipitate phase in the structure.

Keywords: EBM, Ductiliy, Phase analysis.

1. Introduction

With the development of technology, material production methods are also enhancing every day. From the production of metallic materials point of view of the production of metallic materials, these developments are added to the traditional production methods such as additive manufacturing (AM) as a brand new innovative production methods.

The aviation industry requires more resistant, lighter and advanced segments. Additive manufacturing provides more opportunities to address these requirements. To illustrate, it enables more freedom of shape, fewer fastener installation, a much shorter production time, and a cost effective prototyping [1].

These methods that can be used in the production of materials by additive manufacturing are given Figure 1.

Electron beam melting (EBM) is one of the most widely used type of additive manufacturing and it is based on powder bed fusion technologies. EBM process, with its ability to directly machine complex geometries, is well suited for the direct production of complex parts in low volumes. It is possible to complete the production within 24 hours from the completion of the design [3].

Thanks to the electron beam, the powders laid are melted and the next layer of powder is laid again. This process continues layer by layer until the final shape is formed [4]. The parameters that affect production in the EBM process are [5]:

- Layer Thickness
- Beam Current
- Beam Speed
- Line Offset

Fig 1. Classification of AM Technologies [2].

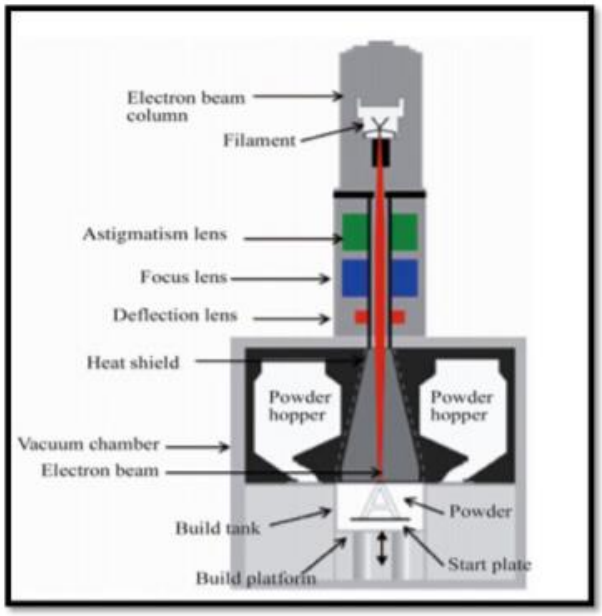

Fig 2. Electron beam melting process [4].

Inconel alloys are Ni-based superalloys and out of these type of alloys Inconel 718 is the most commonly used superalloys owing to superior mechanical properties at high temperature (up to 650℃ − 700 ℃); high strength, high creep and corrosion resistance. This alloy contains some elements such as Nb, Mo, Al, and Ti which upon heat treatment precipitate as hard phases improving the alloy's strength and hardness [6]. IN718 shows main γ (NiCr - face centered cubic) matrix and some intermetallic precipitation phases;

- γ′ (Ni_3AlTi - body centered tetragonal)
- γ′′(Ni_3Nb - body centered tetragonal)
- δ (Ni_3Nb - orthorhombic)
- MC
- Laves ($(Ni, Fe, Cr)_2$(Nb,Mo,Ti))

The composition of the alloy leads to more γ′′ phase than γ′ phase in the structure. It is stated in the literature that as the amount of niobium in the alloy increases, the γ′′ phase increases [7]. Phases γ′′ and δ have the same composition and can be converted into each other. When the γ′′ phase is exposed to temperatures above 650 ℃, it can transform into the stable γ′′ harmful δ phase [8].

The aim of the study is to understand the changes in the ductility behavior of Inconel 718 material produced by the electron beam method, which is one of the AM methods, by evaluating them within the scope of microstructure and phase analysis.

2. Powder properties and manufacturing part

In the EBM method, powder bed system is used, therefore, the type and properties of powders greatly affect the properties of the final part. Plasma atomized Inconel 718 powder (with a size distribution ranges from 45 to 106 μm) was used for this study. The chemical composition of the powder is given in Table 1.

Table 1. Chemical composition of plasma atomized Inconel 718 powder.

Element	Cr	Fe	Nb	Mo	Ti	Cu	Al	C	Ni
Weight (%)	18.64	18.5	5.15	2.92	0.97	0.1	0.53	0.04	Balance

The powder particles were highly spherical in shape and a few of them were attached with fine satellite contained minimal internal porosity as illustrated in Figure 4.

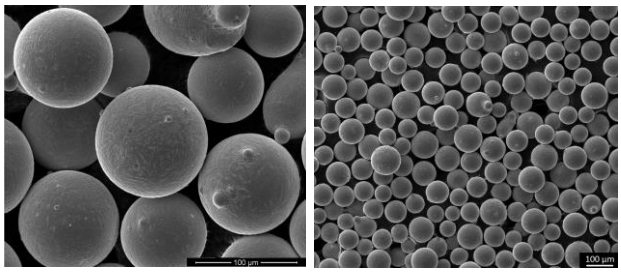

Fig 4. SEM image of powders used in production.

An Arcam A2X EBM system with a gun-accelerating voltage of 60 kV was used to fabricate samples in this study. EBM Control 4 software was utilized along with zigzag pattern scanning strategy for the standard melt theme of Inconel 718. The manufacturing process started after the powder bed was pre-heated to 1023 °C, and this temperature was kept constant throughout the process as suggested in a previous study [9]. During the process, the layer thickness and line offset were fixed at 75 and 125 μm, respectively [10].

After the EBM production, the samples were subjected to the hot isostatic pressing (HIP) before being heat treated according to the AMS 5662 which comprises a solutionizing and two-step aging [11]. HIP at 1200°C for 4 hours at 150 MPa was applied to reduce microstructural inhomegenity and as-built porosity. Archimedes' results showed that samples were free of porosity after HIP and heat treatment.

3. Experimental Part

For the tensile test of the materials produced by the EBM method, the samples were produced by machining in accordance with the ASTM E8 standard. While it is possible to measure in 5 different sample sizes according to the standard, the tensile test was made in the size of the specimen shown in figure 5.

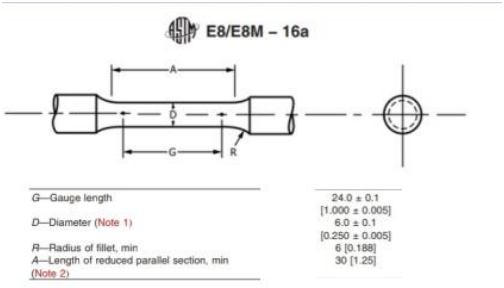

Fig 5. ASTM E8 Specimen Dimensions [12].

The tensile test for the determination of mechanical properties was carried out using a tensile tester (Zwick/Roell Z100 and MacroXtens Extensometer). After tensile stress the fracture surface was examined in a stereo microscope (Nikon SMZ 1000) at macro size and a scanning electron microscope (Zeiss Supra 50 VP) at high magnifications for microscopic examination. In addition, elemental analysis was performed on the EDS module in the SEM under 20 kV accelerating voltage. For phase analysis, X-ray diffraction method (Rigaku Miniflex 600) was used.

4. Results and discussion

4.1. Tensile test results

From the stress-strain curve resulting from the tensile test, emerge many mechanical values such as yield stress, ultimate tensile stress and elongation can be calculated. The results of the 1st specimen were fixed as 100% and the other results were proportionally shown in the graph.

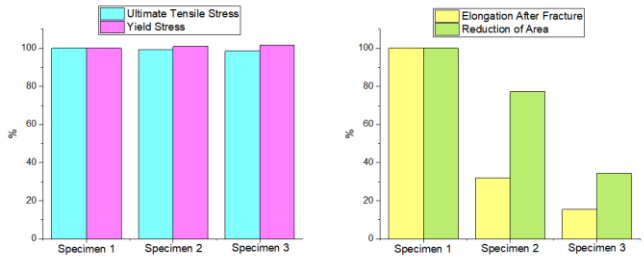

Fig 6. Tensile test results.

In the table shown above, ultimate tensile and yield stress values are similar from sample to sample, whereas great differences were observed in the reduction of area and elongation after fracture values in different samples.

4.2. Failure analysis

After seeing the difference in ductility behavior, the fracture surface was started to be examined in order to understand the reason. Firstly, examinations were carried out in the stereo microscope at macro scale (Figure 7). In these examinations, regions containing different phases were observed in the microstructure in samples with low elongation (Fig. 7 b and c). These regions appear in different colors in Figure 7 and highlighted with red circles.

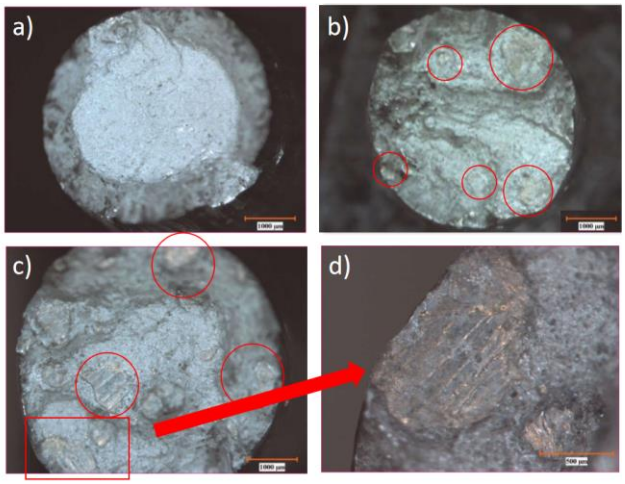

Fig 7. Stereo-microscope images of fracture surface of (a)Specimen 1 (b)Specimen 2 (c,d) Specimen 3.

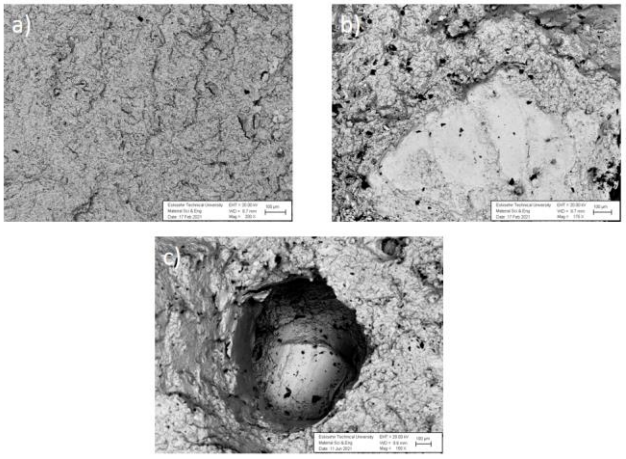

Fig 8. SEM backscatter fracture surface images of (a)Specimen 1 (b)Specimen 2 (c) Specimen 3.

In order to identify the phases showing different contrast in the stereo microscope, SEM images were obtained from the fracture surfaces (Figure 9). In these images, flat regions and dimples were observed in the samples of the samples with a large decrease in ductility values. In the literature, it is clearly stated that a flat fracture is a brittle fracture.

In Figure 9, images at high magnifications are given for two different regions around the dimple in sample number 3.

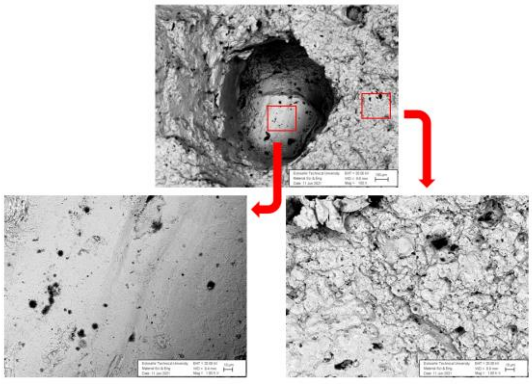

Fig 9. Fracture surface of specimen 3.

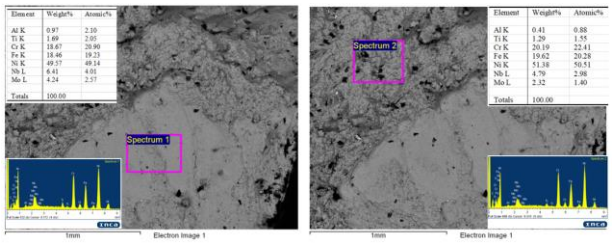

Fig 10. Specimen 2 EDS results.

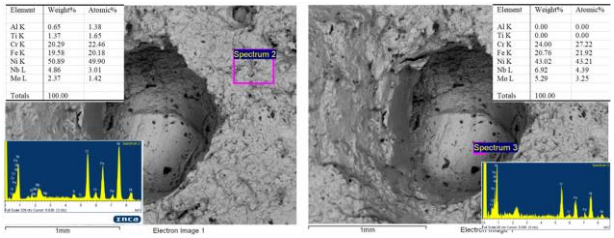

Fig 11. Specimen 3 EDS results.

Table 2. Functions of Alloying Elements in Nickel Superalloys [13].

Alloying element	Function
Chromium	Solid solution strengthening; corrosion resistance
Molybdenum	Solid solution strengthening; creep resistance
Tungsten	Solid solution strengthening; creep resistance
Cobalt	Solid solution strengthening
Niobium	Precipitation hardening; creep resistance
Aluminium	Precipitation hardening; creep resistance
Carbon	Carbide hardening; creep resistance

The EDS results of samples 2 and 3 with different images on the fracture surface are shown in figures 10 and 11. In both structures, a higher rate of niobium was observed in the regions thought to have broken brittle compared to other regions. As can be seen in Table 2, niobium has a precipitation hardening effect in nickel superalloys. Moreover, the polished surface, except for the fracture surface, was examined in EDS analysis.

In Figure 11, the image taken from the as-polish surface at 10.000X magnification and the point elemental analysis made from the white regions, 18 at % niobium was found. This is corresponding to 4 times incerease in comparison to main material. As a result of EDS mapping performed to understand whether this situation is present in the general structure, abundant niobium was observed in all white areas.

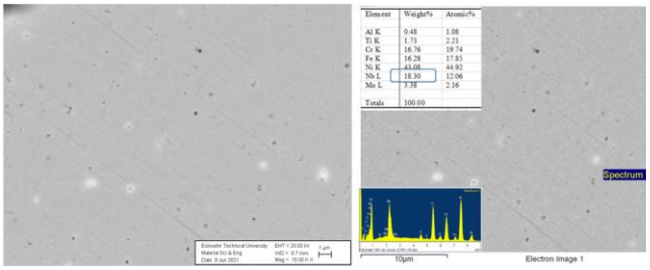

Fig 12. EDS point analysis from the white regions of as-polished sample.

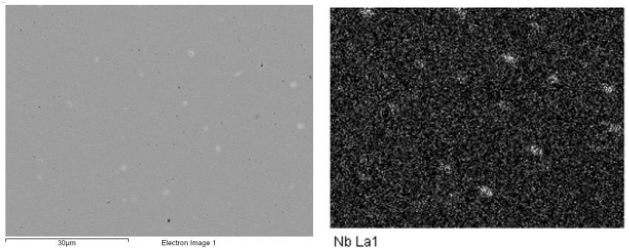

Fig 13. Nb EDS mapping of as-polished sample.

In addition to the evaluation of elemental analysis results, phase analysis was performed with X-Ray Diffraction for a more accurate evaluation of the results. In the XRD experiments, examination could not be made directly from the fracture surface since XRD requires flat surfaces. For XRD experiments flat samples were cut from the tensile sample.

Measurements for all 3 samples were taken between 20-100 2θ° at a rate of 2°/minute. While more counts were collected from the first peak of the main matrix in the sample having a high ductility value, more signals were collected from the second peak, including the precipitate phase, in the other two samples. Although similar differences were observed the layered Inconel 718 produced in different directions in the literature, it is thought that the difference observed in this study is not due to the orientation since all the materials examined within the scope of this damage analysis were in the z direction.

When these two peaks are examined, another difference is that while only the main matrix phase (NiCr - face centered cubic) is found in the first peak (111), there is a precipitate phase (Ni_3Nb - body centered tetragonal) overlapping in the second peak.

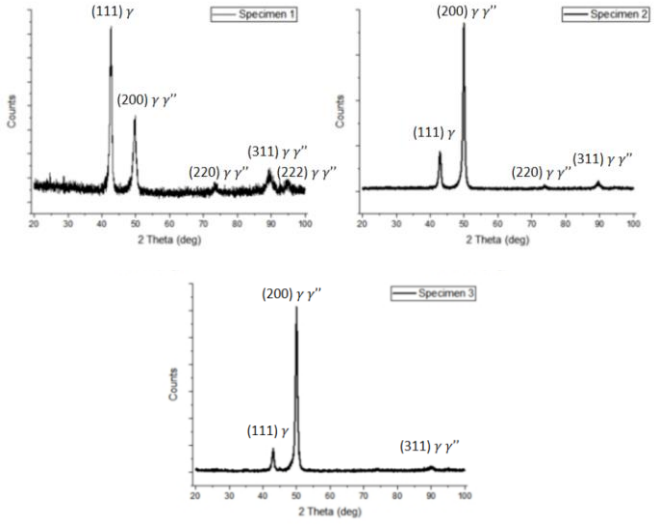

Fig 14. XRD Analysis of all the samples.

5. Conclusions

- Similar to conventional methods, the amount of Nb in IN718 produced by the EBM method is of great importance in ductility behavior.

- The regions containing high amounts of Nb were found in EDS analysis. The active precipitate phase was determined as γ'' (Ni_3Nb). This phase is directly related to the amount of Nb in the material. Nb, which is at the level of 5 at % in powder content, increased up to 18 at % locally.
- The negative effect of MC is known, but the unexpected phase was not observed in the XRD analysis performed in this study.
- The change in ductility behavior was observed in parallel for the reduction of area and elongation after fracture values.

Future Works

In the future studies, the positions of the samples produced during production can be controlled and the conditions caused by factors such as air flow in the furnace and cooling rate can be examined. The same examinations can be repeated for new samples using different HIP parameters during production. Detailed transmission electron microscopy can be used to the to understand the exact chemistry and texture effect.

Acknowledgments

This study is carried out as a project of the Presidency of Defense Industry. The equipments of Tusas Engine Industry and Eskisehir Technical University were used in the research.

Author's statement

Conflict of interest: Authors state no conflict of interest. Informed consent: Informed consent has been obtained from all individuals included in this study. Ethical approval: The research related to human use complies with all the relevant national regulations, institutional policies and was performed in accordance with the tenets of the Helsinki Declaration, and has been approved by the authors' institutional review board or equivalent committee.

References

1. Kumar, L. J., & Nair, C. K. (2017). Current trends of additive manufacturing in the aerospace industry. In Advances in 3D printing & additive manufacturing technologies (pp. 39-54). Springer, Singapore.

2. ASTM F2792-12a, Standard Terminology for Additive Manufacturing Technologies, (Withdrawn 2015), ASTM International, West Conshohocken, PA, 2012, www.astm.org

3. Larsson, M., Lindhe, U., & Harrysson, O. L. A. (2003). Rapid manufacturing with Electron Beam Melting (EBM)-A manufacturing revolution?. In 2003 International Solid Freeform Fabrication Symposium.

4. Azam, F. I., Rani, A. M. A., Altaf, K., Rao, T. V. V. L. N., & Zaharin, H. A. (2018, March). An in-depth review on direct additive manufacturing of metals. In IOP Conference Series: Materials Science and Engineering (Vol. 328, No. 1, p. 012005). IOP Publishing.

5. Pushilina, N., Syrtanov, M., Kashkarov, E., Murashkina, T., Kudiiarov, V., Laptev, R., ... & Koptyug, A. (2018). Influence of manufacturing parameters on microstructure and hydrogen sorption behavior of electron beam melted titanium Ti-6Al-4V alloy. Materials, 11(5), 763)

6. Sharma, S. K., Biswas, K., Nath, A. K., Manna, I., & Majumdar, J. D. (2020). Microstructural characterization of laser surface-melted Inconel 718. Journal of Optics, 49(4), 494-509.

7. Amato, K. N., Gaytan, S. M., Murr, L.E., Martinez, E., Shindo, P.W., Hernandez, J., ... & Medina, F. (2012). Microstructures and mechanical behavior of Inconel 718 fabricated by selective laser melting. *Acta Materialia,* 60(5), 2229-2239

8. Hong, S. J., Chen, W. P., & Wang, T. W. (2001). A diffraction study of the γ ″phase in INCONEL 718 superalloy. *Metallurgical and Materials Transactions A*, *32*(8), 1887-1901.

9. Karimi, P., Sadeghi, E., Ålgårdh, J., & Andersson, J. (2019). EBM-manufactured single tracks of Alloy 718: Influence of energy input and focus offset on geometrical and microstructural characteristics. *Materials Characterization*, *148*, 88-99.

10. Kirka, M. M., Unocic, K. A., Raghavan, N., Medina, F., Dehoff, R. R., & Babu, S. S. (2016). Microstructure development in electron beam-melted Inconel 718 and associated tensile properties. *Jom*, *68*(3), 1012-1020.

11. Qi, H., Azer, M., & Ritter, A. (2009). Studies of standard heat treatment effects on microstructure and mechanical properties of laser net shape manufactured Inconel 718. *Metallurgical and Materials Transactions A*, *40*(10), 2410-2422.

12. ASTM E8 / E8M-21, Standard Test Methods for Tension Testing of Metallic Materials, ASTM International, West Conshohocken, PA, 2021, www.astm.org

13. Mouritz, A. P. (2012). Introduction to aerospace materials, Superalloys for gas turbine engines, p. 258. Elsevier.